Conductivity Relaxation of 1-Methyl-2-pyrrolidone-Plasticized Polyaniline Film

Hsun-Tsing Lee, Kuen-Ru Chuang, and Show-An Chen*

Department of Chemical Engineering, National Tsing Hua University, Hsinchu 30043, Taiwan, ROC

Pei-Kuen Wei,† Jui-Hung Hsu,‡ and Wunshain Fann†,‡

Institute of Atomic and Molecular Sciences, Academia Sinica, P.O. Box 23-166, Taipei 10764, Taiwan, ROC, and Department of Physics, National Taiwan University, Taipei 10764, Taiwan, ROC

Received February 22, 1995; Revised Manuscript Received September 5, 1995®

ABSTRACT: The conductivity relaxation of 1-methyl-2-pyrrolidone (NMP)-plasticized polyaniline (PAn) film was measured using dielectric analysis (−50 to +250 °C, 0.4−10^5 Hz). The complex electric modulus (M^*) representation of the results of dielectric measurement of NMP-plasticized PAn film exhibits two relaxation peaks, which is contrary to the single relaxation peak of the PAn powder (free from NMP). This implicates a two-phase interwoven network structure of the film, which is supported by the results from UV−vis spectroscopy (−50 to +250 °C) and near-field scanning optical microscopy of the NMP-plasticized PAn film and from the conductivity relaxations of the model compounds: the fully oxidized and fully reduced forms of PAn powder. The peak at lower frequency is due to the conductivity relaxation of the phase with oxidized repeat units and that at higher frequency to the relaxation of the phase with reduced repeat units. The conductivity of the phase of reduced repeat units is higher than that of the phase of oxidized repeat units.

Introduction

Polyaniline (PAn) is an environmentally stable conducting polymer with a high conductivity on the order of 10^0 S/cm after doping.[1,2] The PAn base consists of equal numbers of reduced [−(C_6H_4)NH(C_6H_4)NH−] and oxidized [−(C_6H_4)N=(C_6H_4)=N−] repeat units. The PAn hydrochloride powder synthesized in aqueous HCl is insoluble in common organic solvents and even in 1-methyl-2-pyrrolidone (NMP), which is the only organic solvent found so far that can dissolve high molecular weight PAn. However, PAn base, which can be obtained by treating PAn hydrochloride with aqueous NH_4OH,[3] is soluble in NMP and can be cast into a flexible film[4−8] with residual NMP as plasticizer. During film casting, NMP is very difficult to remove completely. The resulting PAn film usually contains a considerable amount of NMP, about 10−18% by weight,[5,9,10] and was termed NMP-plasticized PAn (designated as NMP-p-PAn) film.[9] This is due to the high boiling point of NMP (202 °C) and the presence of the hydrogen-bonding interaction of the C=O group in NMP with the NH group in PAn.[9,11]

The effects of NMP on the structure and doping behavior of PAn investigated by us[9] indicated that the presence of NMP can lead to a smooth and dense surface morphology and therefore to a limited specific surface area for dopant diffusion. Futhermore, the hydrogen-bonding interaction of the C=O group in NMP with the proton in a protonic acid dopant can interfere with the doping of PAn by the acid. Thus, doping of the film by the usual immersion in a dopant solution can only result in a doping in the vicinity of the film surface.[9]

The relaxation of an electric field in a charge carrier system results from the charge hopping of mobile carriers over potential barriers, which can lead to short-range (or local) ac conductivity and long-range dc conductivity. The conductivity relaxation in conjugated polymers arising from carrier hopping is different from the dielectric relaxation arising from permanent dipole reorientation in conventional polymers. Based on dielectric relaxation measurements, it was found that for poly(arylenevinylene)s,[12] poly(3-octylthiophene) (P3OT),[13] and PAn powder,[14] the electric field decay function can be described by the nonexponential decay function exp[−(t/τ_p)$^\beta$], where β is a parameter characterizing the relaxation time distribution and τ_p the characteristic conductivity relaxation time. For P3OT, the conductivity relaxation time distribution varies with temperature levels and is highly related to molecular motion. In the glassy region, side chain motion gives no significant effect on charge transport, while in the glass transition and rubbery regions, the relaxation time distribution becomes broadened with temperature. As the coplanar subchains in the ordered region melt, the conjugation length decreases and its distribution becomes narrower. For PAn powder, the relaxation time distribution becomes narrower as the cross-linking reaction occurs at elevated temperatures.[14]

This work is undertaken to characterize the NMP-p-PAn film by dielectric measurement, UV−vis spectroscopy, and near-field scanning optical microscopy (NSOM). It is found that NMP can induce a two-phase structure in the NMP-p-PAn film.

Experimental Section

1. Chemicals. Aniline and hydrochloric acid were synthetic grade from Merck. Synthetic grade NMP was from Ferak Co., Germany. The PAn hydrochloride powder was synthesized by the oxidative polymerization of anline in 1 M aqueous HCl with $(NH_4)_2S_2O_8$ as oxidant as described in our previous work,[9] which is similar to the method used by MacDiarmid *et al.*[15] The powder was converted to PAn base (an emeraldine base) by treatment with 1 M aqueous NH_4OH followed by drying under dynamic vacuum.

The fully reduced form of PAn (R-PAn) powder was prepared following a method similar to that of Wang *et al.*[16] by reduction

* Author to whom correspondence should be addressed.
† Institute of Atomic and Molecular Sciences, Academia Sinica.
‡ Department of Physics, National Taiwan University.
® Abstract published in *Advance ACS Abstracts,* October 15, 1995.

0024-9297/95/2228-7645$09.00/0

of PAn base with hydrazine in anhydrous ethanol solution under a nitrogen atmosphere for 2 days. The ethanol and excess hydrazine after the reaction were removed in a rotary evaporator under reduced pressure. The white R-PAn powder was dried under dynamic vacuum and then stored in a sealed sample tube filled with argon. The fully oxidized form of PAn (O-PAn) powder was prepared following the method of MacDiarmid and co-workers[17] by an oxidation of PAn base with *m*-chloroperbenzoic acid in NMP solution under a nitrogen atmosphere for 20 min. The dark purple O-PAn powder was reprecipitated in methanol and filtered on a Buchner funnel. The precipitate was washed with acetone and diethyl ether. The O-PAn so obtained was then dried under dynamic vacuum and stored in a vacuum desiccator. The structures of the present PAn base, R-PAn, and O-PAn were examined by IR and UV–vis spectroscopies and found to be identical to those reported in the literature.[18-21]

The PAn film was prepared by casting PAn solution in NMP on a Petri dish and drying under dynamic vacuum at 50–60 °C. The resulting film contained a considerable amount of NMP, about 10–18% by weight. The film is designated as NMP-plasticized PAn (NMP-p-PAn) film. The process proposed by Wei and co-workers[10] was used to prepare the NMP-free film. First, the NMP-p-PAn film was doped with HCl by immersing the film in 1 M aqueous HCl for 18 h at room temperature. The resultant film was then undoped to its base form by immersing the film in 1 M aqueous NH_4OH for 18 h at room temperature. This doping–undoping cycle was repeated four times to obtain a film containing about 2 wt % NMP as determined by TGA measurement.

2. Characterization. A thermogravimetric analyzer (TGA; Perkin-Elmer Model TGS-2) was used to measure weight loses of PAn films under a nitrogen stream during a temperature scan from 50 to 600 °C with a heating rate of 10 °C/min.

A dynamic mechanical analyzer (DMA; DuPont Model 983) was used to measure the flexural and loss moduli (E' and E'') of a cast film of PAn in the temperature range −140 to +250 °C with a heating rate of 2 °C/min and a frequency of 1 Hz. The size of the specimens was about 20 mm long, 3 mm wide, and 0.11 mm thick. After mounting a specimen in the sample chamber, the specimen length subject to cyclic flexural motion was about 1 mm.

An ultraviolet recording spectrophotometer (UV–vis; Shimadzu Model UV-160) was used to measure optical absorbances in the wavelength range 200–1100 nm of a solid film coated on a glass plate. The spectrophotometer was equipped with a variable-temperature cell to allow for measurement of spectra under a nitrogen stream from −100 to +250 °C; the soaking time was 10 min at each specific temperature, and the heating rate used was about 1–2 °C/min.

A dielectric analyzer (DuPont Model DEA 2970, frequency range $0.03–10^5$ Hz) was used to measure the dielectric constant ϵ' and dielectric loss ϵ'' of tablets of O-PAn, R-PAn, and PAn (free from NMP) and of the NMP-p-PAn film in the frequency range $0.4–10^5$ Hz and the temperature range −50 to +250 °C under nitrogen gas purging. The tablets of the polyanilines were prepared by compressing their powders under a pressure of 2.94×10^7 Pa at room temperature. The sample sizes were about diameter 25 mm × thickness 0.4 mm for the tablets and 25 mm × 25 mm × 0.16 mm for the films. During the DEA measurements, the specimens were placed between two sensors under a 300 N force.

A transmission-mode near-field scanning optical microscope (NSOM) operated at two different wavelengths was used to examine the morphology of NMP-p-PAn in the submicron scale. The details of the instrumentation design of the NSOM will be published elsewhere.[22] The key elements in this NSOM are metal-coated tapered fiber probes[23] and shear-force feedback.[24] The tapered fiber had a tip diameter of 100 nm, which was coated with 75 nm thick aluminum. The incident light was either from a 5 mW red He–Ne laser (632.8 nm) or a 0.5 mW green He–Ne laser (543.5 nm). These lasers were coupled into the tapered fiber probe to serve as the near-field optical sources. The shear-force feedback was used to maintain the tip and sample separation within 100 Å. In the shear-force technique, the fiber probe was set into vibration near its resonance frequency and the vibrational amplitude was measured by the beam diffraction method.[25] As the tip approached the sample, the amplitude was decreased because of the attractive force between the tip and the sample surface. This shear-force signal was sent to the sample PZT scanning stage to regulate the tip–sample distance. During scanning, the feedback signal generated a topographic image, which is important in decoupling the optical information with the topographic properties. Hence a topographic and an optical image can be simultaneously obtained by this NSOM. In recording the transmission-mode optical image, the optical signal traveling through the sample was reflected at a right angle by a mirror placed directly below the sample. A long working distance objective was used to focus the light on a photomultiplier tube (PMT), and the signal from the PMT was sent to a lock-in amplifier. The signal to noise ratio of this transmission-mode NSOM was about 100, which ensures the capability of distinguishing the small absorption variation in the NMP-p-PAn film.

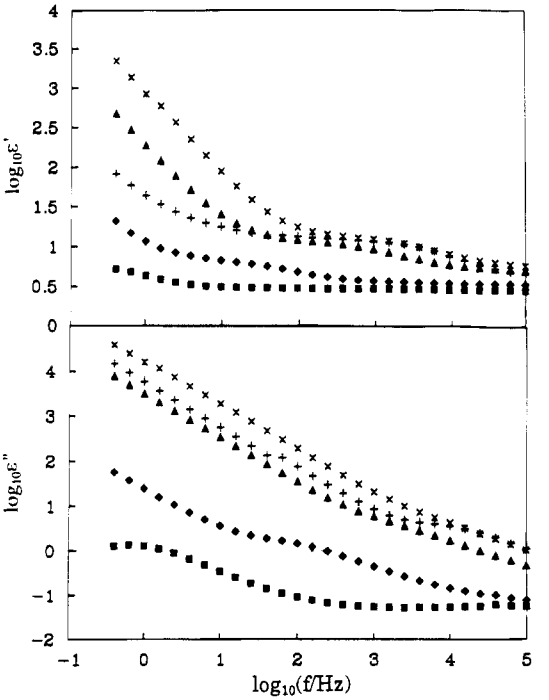

Figure 1. (a) Dielectric constant ϵ' and (b) dielectric loss ϵ'' vs log f for the NMP(16 wt %)-plasticized PAn film at 0 (■), 50 (◆), 80 (▲), 100 (×), and 200 °C (+).

Results and Discussion

1. Electric Modulus Analysis. The real and imaginary parts of the complex permittivity ϵ^*, the dielectric constant ϵ', and the dielectric loss ϵ'' versus frequency for the NMP(16 wt %)-p-PAn film at five representative temperatures in the temperature range from 0 to 200 °C are shown in Figure 1. Both ϵ' and ϵ'' increase with decreasing frequency at all tempoerature levels. The ϵ'' exhibits no loss peaks even at higher temperature and increases about linearly with decreasing frequency due to the increased contribution of dc conductivity, while ϵ' increases sharply with decreasing frequency below 10^2 Hz. The strong low-frequency dispersion for ϵ' and without loss peak for ϵ'' are the characteristics of charged carrier systems.[26] The localized charge carriers under an applied alternating electric field can hop to neighboring localized sites like the reciprocating motion of a jumping dipole or can jump to neighboring sites which form a continuous connected network, allowing the charges to travel through the entire physical dimensions of the sample and causing the electric

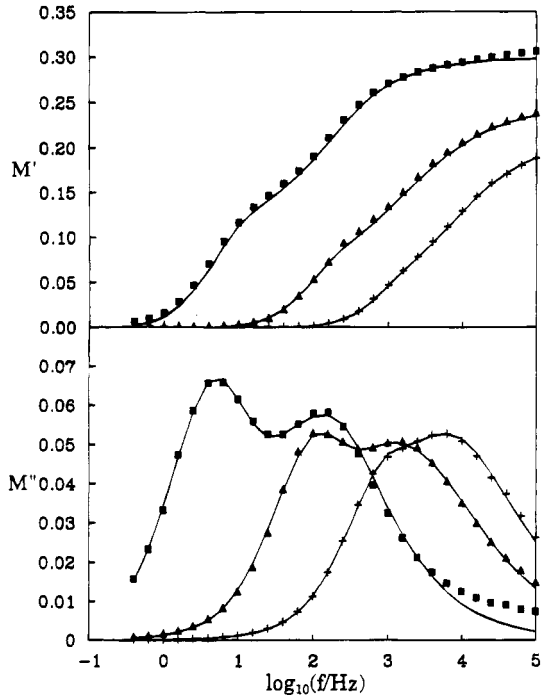

Figure 2. (a) Real part M' and (b) imaginary part M'' of the complex electric modulus M^* vs log f for the NMP(16 wt %)-plasticized PAn film at 50 (■), 70 (▲), and 90 °C (+).

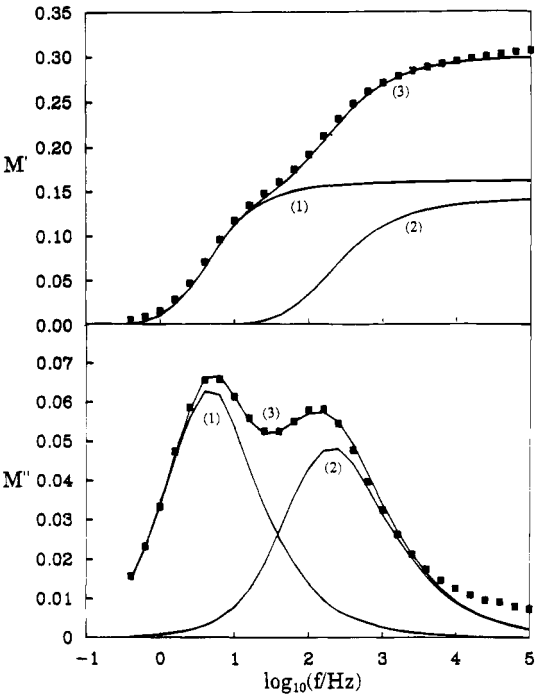

Figure 3. Analysis of M' and M'' for the NMP(16 wt %)-plasticized PAn film at 50 °C: (■) experimental data; curve 1 represents the contribution from the phase of oxidized repeat units, curve 2 from the phase of reduced repeat units, and curve 3 the combination of (1) and (2).

conduction. Both processes suffer a time delay response in the applied alternating electric field. During the motion of charge carriers, the applied electric field E will be subject to a decay. Such relaxation of E is termed electric field relaxation,[21] and the relaxation of the charge carrier system is termed conductivity relaxation.

In order to analyze the conductivity relaxation of the NMP-p-PAn film, the complex permittivity is converted to the complex electric modulus $M^*(\omega)$, according to the relation defined by Macedo *et al.*[27] The real and imaginary parts M' and M'' of the electric modulus can be calculated from ϵ' and ϵ'' via

$$M' = \frac{\epsilon'}{\epsilon'^2 + \epsilon''^2}$$

$$M'' = \frac{\epsilon''}{\epsilon'^2 + \epsilon''^2} \qquad (1)$$

M' and M'' of the NMP-p-PAn film converted from ϵ' and ϵ'' by eq 1 are shown in Figure 2. M' approaches zero at low frequencies, indicating that the electrode polarization gives a negligible contribution to M' and can be ignored when the permittivity data are expressed in this form.[27] Each M'' curve exhibits two relaxation peaks at the lower characteristic relaxation frequency $f_{max,L}$ and higher characteristic relaxation frequency $f_{max,H}$. The dispersions of M' and M'' indicate a presence of relaxation time distribution of conduction. The electric modulus M is a more convenient term in characterizing a decay of an applied electric field E due to charge motion in a conductor than ϵ, since M ($\equiv 1/\epsilon \equiv E/D$) is proportional to E, where D is the dielectric displacement.[26] As a constant voltage is applied on the sample, the electric field in the sample decays as a function of time as $E(t) = E(0)\varphi(t)$, where $E(0)$ is the initial electric field and $\varphi(t)$ is the decay function. In the frequency domain, the electric field relaxation can be expressed by[28]

$$M^* = M' + iM'' = M_\infty\left\{1 - \int_0^\infty dt\, \exp(-i\omega t)\left[\frac{-d\varphi(t)}{dt}\right]\right\} \qquad (2)$$

where M_∞ is the high-frequency limit of inverse ϵ' defined as $M_\infty = 1/\epsilon_\infty$, and ω is the angular frequency. For describing condensed matter with a non-Debye relaxation, the Kohlrausch–Williams–Watts (KWW) nonexponential decay function[29]

$$\varphi(t) = \exp[-(t/\tau_p)^\beta], \qquad 0 < \beta \le 1 \qquad (3)$$

can be used satisfactorily, where τ_p is the characteristic conductivity relaxation time and β is a parameter characterizing the relaxation time distribution. When $\beta = 1$, the decay is exponential with a single conductivity relaxation time. When β decreases, the width of the relaxation time distribution increases.

2. Deconvolution and Assignment of Conductivity Relaxation Time Distribution. The bimodal distribution of M'' vs log f for the NMP-p-PAn film can be deconvoluted into two components, with each analyzed by the techniques developed by Moynihan *et al.*[28] using the relaxation parameters M_∞, τ_p, and β as fitting parameters for each component. The two components and their summations at 50 and 100 °C of M' and M'' are shown in Figures 3 and 4, respectively. The deviation between the fitting curves (solid lines in Figure 2 and curve 3 in Figures 3 and 4) and the data is small. The dispersion or shape of the M'' curves depends on the value of β; greater deviation of β from 1 indicates a larger dispersion. While the position of the peak depends on τ_p, a large τ_p gives a low characteristic relaxation frequency f_{max} ($f_{max} = 1/2\pi\tau_p$).

Each of the M'' curves of the NMP-p-PAn film exhibits two relaxation peaks, which is contrary to the single

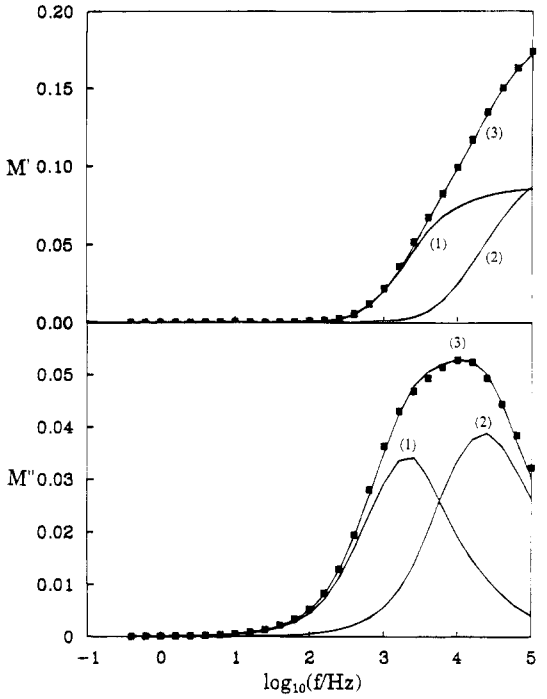

Figure 4. Analysis of M' and M'' for the NMP(16 wt %)-plasticized PAn film at 100 °C: (■) experimental data; curve 1 represents the contribution from the phase of oxidized repeat units, curve 2 from the phase of reduced repeat units, and curve 3 the combination of (1) and (2).

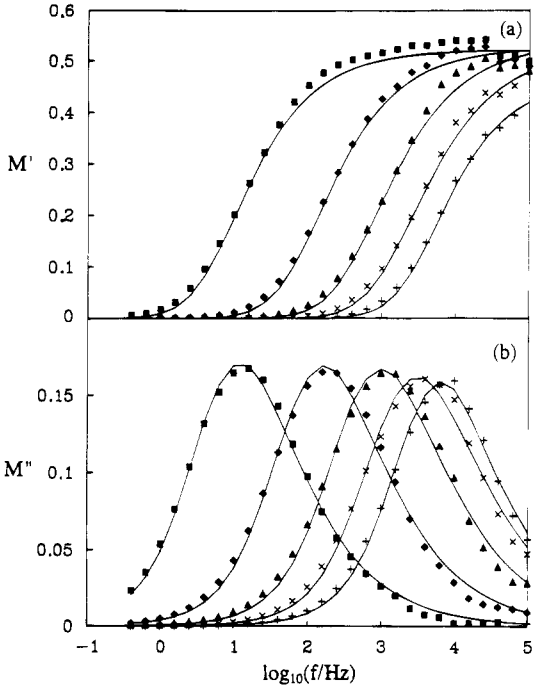

Figure 5. (a) Real part M' and (b) imaginary part M'' of the complex electric modulus M^* vs log f for the PAn powder at 20 (■), 70 (◆), 120 (▲), 160 (×), and 200 °C (+).

relaxation peak of the PAn powder (free from NMP) indicated in Figure 5, though the variations of both ϵ' and ϵ'' with frequency for the PAn powder are similar to those for the film and ϵ'' exhibits no loss peaks in the frequency range $0.4-10^5$ Hz.[14] The occurrence of two relaxation peaks is not caused by any crystalline structure in the NMP-p-PAn film because the film is amorphous, which was examined by Wei *et al.*[10] and us[9] using wide-angle X-ray diffraction analysis; it is considered to be due to the two-phase structure in the film

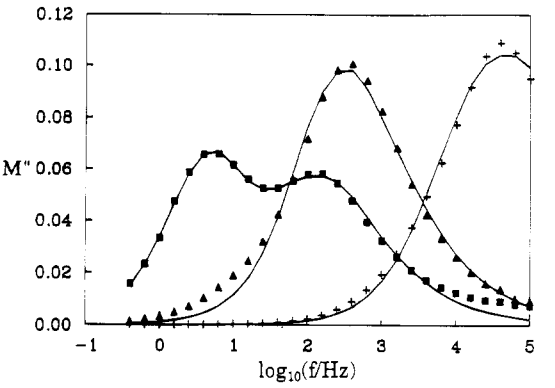

Figure 6. Imaginary part M'' of the complex electric modulus M^* vs log f for the NMP(16 wt %)-plasticized PAn film (■), O-PAn (▲), and R-PAn (+) at 50 °C.

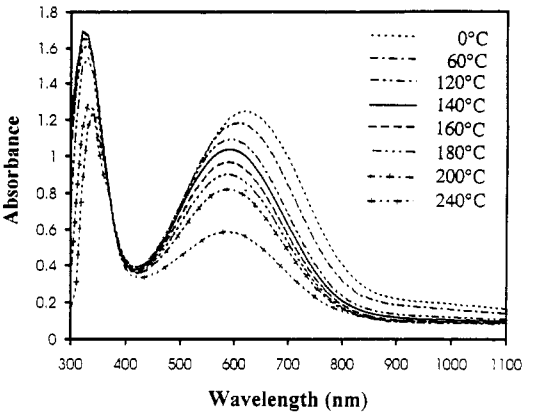

Figure 7. UV–vis absorption spectra of the NMP(16 wt %)-plasticized PAn film at various temperatures from 0 to 240 °C.

as described below. The M'' vs log f curves for the NMP-p-PAn film, the fully oxidized form of PAn (O-PAn) powder, and the fully reduced form of PAn (R-PAn) powder at 50 °C are shown in Figure 6. The O-PAn and R-PAn powders each have one relaxation peak, which can also be characterized by the nonexponential decay function, eq 3. The two relaxation peaks in the NMP-p-PAn film can be attributed to the phase of oxidized repeat units for the lower frequency peak and the phase of reduced repeat units for the higher frequency peak, as can be inferred from the lower frequency peak of O-PAn than R-PAn. Since O-PAn and R-PAn are easily reduced and oxidized by H_2O and O_2, respectively, they are not cast into films for the dielectric measurements in this work.

UV–vis spectra of NMP-p-PAn thin film at various temperatures in the range 0–240 °C are presented in Figure 7. They also indicate a two-phase structure of the film as described below. The UV–vis spectrum of NMP-p-PAn at room temperature exhibits absorption peaks at 320 and 630 nm, which are due to the $\pi-\pi^*$ transition of the benzenoid rings and exciton absorption of the quinoid rings, respectively.[21,30] A plot of the energies of the absorption maxima of these two peaks versus temperature is shown in Figure 8. Theoretically, the energy for a $\pi-\pi^*$ transition or exciton transition should increase with increasing temperature due to a decreased conjugation of PAn subchains, resulting from increased segmental thermal motion at higher temperature. However, for the NMP-p-PAn film, the energy for the $\pi-\pi^*$ transition increases with increasing temperature below 60 °C and remains constant with further heating; then it decreases rapidly with temperature

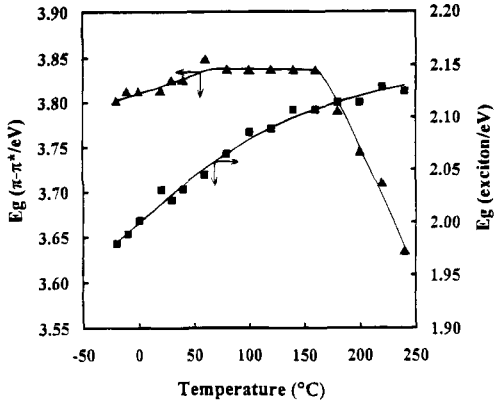

Figure 8. Variations of energy of the absorption maximum E_g of the $\pi-\pi^*$ transition and exciton transition with temperature for the NMP(16 wt %)-plasticized PAn film.

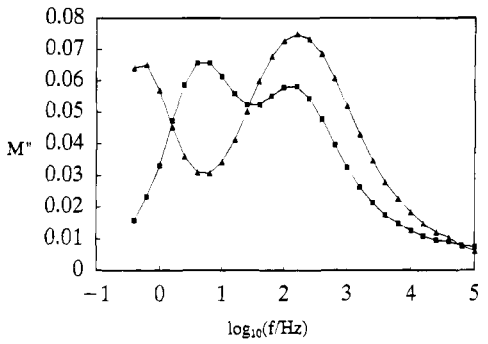

Figure 9. Imaginary part M'' of the complex electric modulus M^* vs log f for the NMP(16 wt %)-plasticized PAn film at 50 °C for the first heating scan (■) and the second heating scan (▲).

above 160 °C. The decrease of energy of $\pi-\pi^*$ transition with increasing temperature is due to the continuous evaporation of NMP as described below. The distortion between the phenyl rings of PAn decreases due to the increase of rigidity of the reduced repeat units resulting from the evaporation of NMP above 120 °C.[9] The π-electrons thus become easier to delocalize as the energy for the $\pi-\pi^*$ transition decreases, implying that the majority of NMP is located in the region of reduced repeat units. The energy of the exciton transition increases with increasing temperature as in other conjugated polymers,[31] implying that only a minor amount of NMP is located in the region of oxidized repeat units. Thus, it can be inferred that the residual NMP in the NMP-p-PAn film is mainly distributed in the region of reduced repeat units, which arises from the hydrogen-bonding interaction of the C=O group in NMP with the NH group in the reduced repeat unit of PAn, as was investigated via IR spectroscopy reported in our previous work.[9] This observation would also indicate the presence of a two-phase structure of the film.

The NMP-p-PAn film was subject to repeated DEA heating scans from −50 to +250 °C to see if the two-phase structure still exists as the NMP content decreases. Before the second scan, the film contains 7 wt % NMP as determined from TGA measurement. The M'' vs long f curves for the NMR-p-PAn film at 50 °C for the first and second heating scans are shown in Figure 9. As the content of NMP is reduced, the phase separation becomes more pronounced as can be seen from the increased sharpness in relaxation spectrum in the second heating scan.

We also attempted to prepare NMP-free PAn films using the method proposed by Wei and co-workers[10] for DEA measurements. After the four doping-undoping cycles, the NMP-p-PAn films curled and contained only about 2 wt % NMP. These nearly NMP-free films were fragile. Upon putting these curled films between the two sensors and applying a 300 N force for DEA measurements, the films were broken into pieces. Owing to the presence of air gaps in these broken films, the DEA results are not reproducible. Since the fragile films cannot be ground into powders, we had no way to press the samples into tablets with smooth surfaces for DEA measurement. Though the peak frequencies and relative peak heights of the two relaxation peaks are not reproducible, the relaxation spectra all exhibit two relaxation peaks. This indicates a presence of the two-phase structure in the NMP(2 wt %)-p-PAn film.

3. Near-Field Scanning Optical Microscopy. The near-field scanning optical microscopy (NSOM) images on the same area of the NMP-p-PAn film (about 800 Å thick) coated on a glass substrate with a thickness of 0.1 mm are shown in Figure 10. We did not attempt to record NSOM images of a NMP-free PAn film, because the NMP-p-PAn film will delaminate from the glass substrate during the doping−undoping cycles proposed by Wei and co-workers.[10] The topographic image (Figure 10a, similar to that obtain using atomic force microscopy[32]) shows that the film surface is uniform; it provides no information on the morphology in the bulk. The optical images with 632.8 nm (red) and 543.5 nm (green) He−Ne laser sources are shown in Figures 10b and c, respectively. These two optical images indicate an existence of the two-phase structure as reflected in the presence of the dark and bright regions and, in addition, nearly opposite contrast of the two images. The ratio of the absorbance at 632.8 nm to that at 543.5 nm at room temperature is about 1.23, as can be estimated from the UV−vis spectra of NMP-p-PAn film in Figure 7. The oxidized repeat units with peak absorbance at 630 nm will absorb 632.8 nm light more efficiently than 543.5 nm light. Thus the bright regions in Figure 10b (or the dark regions in Figure 10c) can be assigned as the reduced repeat unit-rich phase, while the dark regions in Figure 10b (or the bright regions in Figure 10c) can be assigned as the oxidized repeat unit-rich phase; the gray regions contain both reduced and oxidized repeat units. This assignment can also be supported by the fact that the bright and dark regions have sizes greater than 0.1 μm (1000 Å), which is larger than the film thickness, 800 Å. The film with such thickness would not allow a full overlap of the region with oxidized repeat units and that with reduced repeat units.

From the UV−vis spectroscopy measurement, conductivity relaxation analysis, and near-field scanning optical microscopy measurement, it is deduced that there are two phases in the NMP-p-PAn film as induced by the presence of NMP. However, the two-phase structure cannot be observed from the results of dynamic mechanical analyses reported by Wei *et al.*[5,10] and by us;[9] a possible reason is that parts of the thermal transitions of the two phases of the NMP-p-PAn film are overlapped such that only one transition is observed. Additionally, the two-phase structure cannot be observed by direct microscopic observation using scanning electron micrography (SEM) and atomic force microscopy (AFM). The SEM micrograph of the NMP(16 wt %)-p-PAn film exhibits a smooth and featureless surface

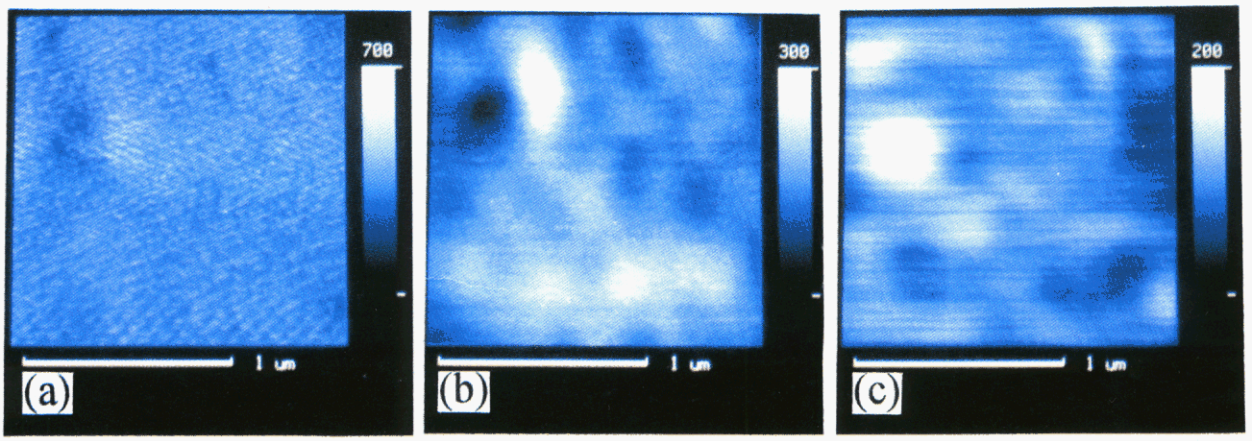

Figure 10. Micrographs from transmission mode near-field scanning optical microscopy (NSOM): (a) topographic image with height ruggedness scale 700 Å; (b) the optical image with a 632.8 nm light source and an arbitrary intensity scale 300; (c) the optical image with a 543.5 nm light source and an arbitrary intensity scale 200.

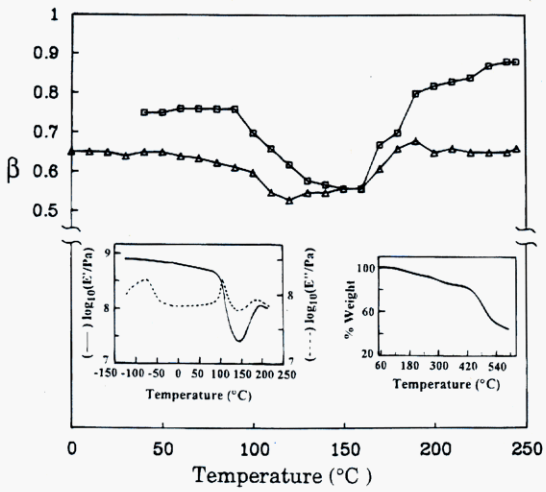

Figure 11. Variations of relaxation time distribution parameter β with temperature for the phase of oxidized repeat units (□) and the phase of reduced repeat units (△) of the NMP(16 wt %)-plasticized PAn film. The inserts at the left and right are the results of the dynamic mechanical (taken from our previous work[9]) and thermogravimetric analyses, respectively, of this film.

morphology and, after extraction with tetrahydrofuran, a fibrilar morphology,[9] while the AFM image of the film coated on a highly ordered pyrolytic graphite substrate shows aggregates of small globules with a diameter about 0.05 μm.[32] These SEM and AFM images exhibit only the roughness of the film surface and provide no information on phase structure.

4. Conductivity Relaxation Behavior at Various Temperature Levels. The calculated values of β from curve fitting at various temperatures for the low- and high-frequency relaxation peaks of the NMP-p-PAn film are shown in Figure 11. The β of the low-frequency peak is larger than that of the high-frequency peak at any temperature except in the range 150−160 °C, where they are about equal. The relaxation time distribution of the phase with oxidized repeat units is thus narrower than that of the phase with reduced repeat units. The variation of β of each phase with temperature can be divided into three regions. For the phase of reduced repeat units, the three regions are as follows: (i) below 50 °C, β remains constant at a value of about 0.65; (ii) between 50 and 120 °C, it drops moderately; (iii) between 120 and 250 °C, it increases moderately up to 180 °C and then remains constant. For the phase of oxidized repeat units, the three regions are as follows: (i) below 90 °C, β remains constant at a value of about 0.75; (ii) between 90 and 160 °C, it drops rapidly; (iii) between 160 and 250 °C, it increases rapidly up to 190 °C and then slowly. The temperature dependence of β is highly related to the molecular motion in the thermal transition region, as illustrated below.

The inserts of Figure 11 at the left and right are the results of the dynamic mechanical (taken from our previous work[9]) and thermogravimetric analyses, respectively, of the NMP(16 wt %)-p-PAn film. They show the following: (i) below 65 °C, the film is in the glassy state; (ii) between 65 and 150 °C, a glass transition occurs with a peak temperature 105 °C; (iii) evaporation of NMP occurs in two stages: the first from 120 to 240 °C with a weight loss of 8 wt %, and the second from 240 to 420 °C with the same weight loss 8 wt %.

From a comparison among the analyses on the thermal transitions from the results of conductivity relaxation, DMA measurements, and TGA measurements, it is quite clear that the conductivity relaxation behavior is highly related to the molecular motions. Below 50 °C, the film is in the glassy state and the main chains are frozen; each β of the two phases of reduced and oxidized repeat units remains constant, indicating that no segmental motions and therefore no disturbance on charge transport are observed. As the subchains are able to relax (above 50 and 90 °C for the reduced and oxidized repeat units, respectively), the torsion angle between two successive rings increases, leading to a decrease in conjugation and an increase in the barrier height for charge transport. Note that the conjugation of reduced repeat units (not a π-conjugation) could be similar to that of poly(phenylene sulfide), in which the aromatic orbitals overlap with the p-orbitals of the neighboring sulfur atoms.[33] Then the relaxation time distribution is broadened (β decreases).[13] The β's of the phases of reduced and oxidized repeat units decrease in the ranges 50−120 and 90−160 °C, respectively. The overall temperature range 50−160 °C is in reasonable agreement with that of the glass transition determined from the DMA results (65−150 °C). As the temperature increases to above 120 °C, the evaporation of NMP leads to an increase of chain aggregation and to a decrease in ring distortion (due to reduced plasticization effect) of the reduced repeat units. Thus, the interchain and intrachain charge transports are easier, and then the relaxation time distribution is narrowed (β increases). The increase of the β of the phase of oxidized repeat

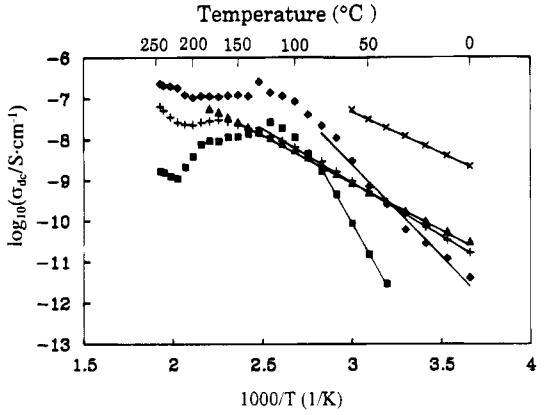

Figure 12. Plots of log σ_{dc} vs $1/T$ for the phase of oxidized repeat units (■) and the phase of reduced repeat units (◆) of the NMP(16 wt %)-plasticized PAn film and powders of O-PAn (▲), R-PAn (×), and PAn (+).

Table 1. Conductivities and Activation Energies of Polyanilines Determined from Dielectric Relaxation Measurement

	σ (S/cm)[d] 40 °C	E_a^{dc} (eV)[e]
O-PAn powder[a]	2.8×10^{-10}	0.46
R-PAn powder[b]	2.0×10^{-8}	0.40
PAn powder	2.8×10^{-10}	0.52
PAn film[c]	(2.9×10^{-12}, 2.6×10^{-10})	(1.53, 0.89)

[a] Oxidized form of polyaniline. [b] Reduced form of polyaniline. [c] The first value in parentheses is obtained from the relaxation peak at lower frequency contributed from the phase with oxidized repeat units, and the second from the peak at higher frequency contributed from the phase with reduced repeat units. [d] Conductivity calculated from DEA data. [e] Activation energy of conduction.

units above 160 °C is also due to the evaporation of NMP.

From the previous discussion, the glass transition of the phase of reduced repeat units starts to occur at 50 °C, while that of the phase of oxidized repeat units starts at 90 °C. Thus, the glass transition of the NMP-p-PAn film occurs first in the phase of reduced repeat units, which contains more NMP than the phase of oxidized repeat units. Both β's of the two phases decrease significantly around the glass transition temperature, 105 °C.[9]

From the conductivity relaxation data, the dc conductivity σ_{dc} can be estimated from the relaxation parameters as[28]

$$\sigma_{dc} = e_0/M_\infty\langle\tau_p\rangle \tag{4}$$

where $\langle\tau_p\rangle$ is the average relaxation time. For a decay function defined by eq 3, $\langle\tau_p\rangle$ is given by[28,34]

$$\langle\tau_p\rangle = \int_0^\infty dt\ \varphi(t) = \frac{\tau_p}{\beta}\Gamma\left(\frac{1}{\beta}\right) \tag{5}$$

where Γ denotes the gamma function. The calculated σ_{dc} for the two phases of the NMP-p-PAn film, PAn powder, and fully oxidized and fully reduced forms of PAn powders are plotted against inverse temperature $1/T$ in Figure 12. Their activation energies of conduction E_a^{dc}, determined from the slopes of the linear portions, together with their conductivities at 40 °C are listed in Table 1. The σ_{dc} of the two phases of the NMP-p-PAn film could be determined independently, inferring that the two phases exist in an interwoven network structure.

Since the σ_{dc} of the O-PAn powder is lower than that of the R-PAn powder in the linear regions, it can be further ascertained that the relaxation peaks at low and high frequency (which correspond to a low and high conductivity, respectively) are due to the relaxations of the phases of oxidized and reduced repeat units, respectively. The E_a^{dc} for the two phases of the NMP-p-PAn film are higher than that for the PAn powder, which results from an increased separation of PAn subchains caused by the presence of NMP.

The σ_{dc} vs $1/T$ plot of the phase of reduced repeat units is linear below 60 °C, and that of the phase of oxidized repeat units is linear below 80 °C. These upper temperature limits of the linear plots are close to the onset temperature, 65 °C, of the glass transition of the NMP-p-PAn film determined from the E'' curve of DMA. Thus, each σ_{dc} vs $1/T$ plot of the two phases of the NMP-p-PAn film follows the Arrhenius plot before the occurrence of the glass transition. The conductivity curves of the phase of reduced repeat units and of the phase of oxidized repeat units exhibit a maximum at 130 and 120 °C, respectively. The temperature at each conductivity maximum of the two phases of the NMP-p-PAn film is higher than the T_g (105 °C), determined from the E'' curve of DMA, by about 15–25 °C. The presence of the conductivity maximum can be attributed to the occurrence of the α relaxation (glass transition) of the PAn subchains as illustrated below. Although the charge mobility increases with increasing temperature, it is compensated by the increased ring distortion in the PAn subchains due to the α relaxation. These two factors compete during the relaxation period. As temperature increases, the latter becomes more important than the former, and the conductivity then drops. Thus, the temperature at the conductivity maximum is higher than T_g as is just the case. The conductivity of the phase of oxidized repeat units decreases more significantly than that of the phase of reduced repeat units above 150 °C. This is due to the occurrence of a cross-linking reaction in the phase of oxidized repeat units.[9,35]

Conclusion

In the NMP-plasticized PAn, the NMP distributes mainly in the region of reduced repeat units, due to the occurrence of hydrogen-bonding interactions of the C=O groups of residual NMP with the NH groups in the reduced repeat units of PAn. The nonuniform distribution of NMP leads to a two-phase structure with interwoven networks as was observed using tranmission-mode near-field scanning optical microscopy. The phase with reduced repeat units has a higher conductivity than that of the phase with oxidized repeat units. As the NMP content is greatly reduced, the PAn film still exhibits the two-phase structure. The conductivity relaxation analysis also provides a method for studying phase separation in blends of two conjugated polymers as well as conductivity in each phase.

Acknowledgment. We wish to thank the National Science Council of ROC for financial aid through project NSC 82-0416-E007-156.

References and Notes

(1) MacDiarmid, A. G.; Epstein, A. J. *Faraday Discuss. Chem. Soc.* **1989**, *88*, 317.
(2) Chen, S. A.; Fang, W. G. *Macromolecules* **1991**, *24*, 1242.
(3) Chiang, J. C.; MacDiarmid, A. G. *Synth. Met.* **1986**, *13*, 193.
(4) Angelopoulos, M.; Ray, A.; MacDiarmid, A. G.; Epstein, A. J. *Synth. Met.* **1987**, *21*, 21.

(5) Wei, Y.; Jang, G. W.; Hsueh, K. F.; Scherr, E. M.; MacDiarmid, A. G.; Epstein, A. J. *Polym. Mater. Sci. Eng.* **1989**, *61*, 916.
(6) MacDiarmid, A. G.; Epstein, A. J. *Faraday Discuss. Chem. Soc.* **1989**, *88*, 317.
(7) Monkman, A. P.; Adams, P. *Synth. Met.* **1991**, *40*, 87.
(8) Cromack, K. R.; Jozefowicz, M. E.; Ginder, J. M.; Epstein, A. J.; McCall, R. P.; Du, G.; Leng, J. M.; Kim, K.; Li, C.; Wang, Z. H.; Druy, M. A.; Glatkowski, P. J.; Scherr, E. M.; MacDiarmid, A. G. *Macromolecules* **1991**, *24*, 4157.
(9) Chen, S. A.; Lee, H. T. *Macromolecules* **1993**, *26*, 3254.
(10) Wei, Y.; Jang, G. W.; Hsueh, K. F.; Scherr, E. M.; MacDiarmid, A. G.; Epstein, A. J. *Polymer* **1992**, *33*, 314.
(11) Chen, S. A.; Lee, H. T. *Synth. Met.* **1992**, *47*, 233.
(12) Bakr, A. A.; North, A. M.; Kossmehl, G. *Eur. Polym. J.* **1977**, *13*, 799.
(13) Chen, S. A.; Liao, C. S. *Macromolecules* **1993**, *26*, 2810.
(14) Lee, H. T.; Liao, C. S.; Chen, S. A. *Makromol. Chem.* **1993**, *194*, 2443.
(15) Asturias, G. E.; MacDiarmid, A. G; McCall, R. P.; Epstein, A. J. *Synth. Met.* **1989**, *29*, E157.
(16) Wang, L. X.; Jing, X. B.; Wang, F. S. *Synth. Met.* **1991**, *41–43*, 685.
(17) Sun, Y.; MacDiarmid, A. G.; Epstein, A. J. *J. Chem. Soc., Chem. Commun.* **1990**, 529.
(18) Tang, J. S.; Jing, X. B.; Wang, B. C.; Wang, F. S. *Synth. Met.* **1988**, *24*, 231.
(19) Wang, L. X.; Jing, X. B.; Wang, F. S. *Synth. Met.* **1991**, *41–43*, 685.
(20) Sun, Y.; MacDiarmid, A. G.; Epstein, A. J. *J. Chem. Soc., Chem. Commun.* **1990**, 529.
(21) Lu, F. L.; Wudl, F.; Nowak, M.; Heeger, A. J. *J. Am. Chem. Soc.* **1986**, *108*, 8311.
(22) Wei, P.-K.; Hsu, J.-H.; Fann, W., paper to be published.
(23) Betzig, E.; Trautman, J. K.; Harris, T. D.; Weiner, J. S.; Kostelak, R. L. *Science* **1991**, *251*, 1468.
(24) Betzig, E.; Finn, P. L.; Weiner, J. S. *Appl. Phys. Lett.* **1992**, *60*, 2484. Toledo-Crow, R.; Yang, P. C.; Chen, Y.; Vaez-Iravani, M. *Appl. Phys. Lett.* **1992**, *60*, 2957.
(25) Grober, R. D.; Harris, T. D.; Trautman, J. K.; Betzig, E. *Rev. Sci. Instrum.* **1994**, *65*, 626.
(26) Jonscher, A. K. *Dielectric Relaxation in Solids*; Chelsa Dielectric Press: London, 1983.
(27) Macedo, P. B.; Moynihan, C. T.; Bose, R. *Phys. Chem. Glasses* **1972**, *13*, 171.
(28) Moynihan, C. T.; Boesch, L. P.; Laberge, N. L. *Phys. Chem. Glasses* **1973**, *14*, 122.
(29) Williams, G. D.; Watts, C. *Trans. Faraday Soc.* **1970**, *66*, 80.
(30) Stafstrom, S.; Bredas, J. L.; Epstein, A. J.; Woo, H. S.; Tanner, D. B.; Huang, W. S.; MacDiarmid, A. G. *Phys. Rev. Lett.* **1987**, *59*, 1464.
(31) Chen, S. A.; Ni, J. M. *Macromolecules* **1992**, *25*, 6081.
(32) Chen, S. A.; Lee, H. T. *Macromolecules* **1995**, *28*, 2858.
(33) Elsenbaumer, R. L.; Shacklette, L. W. In *Handbook of Conducting Polymers*; Skotheim, T. A., Ed.; Marcel Dekker Inc.: New York, 1986; Vol. 1, p 245.
(34) Douglas, R. W. In *Amorphous Materials*; Douglas, R. W., Ellis, B., Eds.; Wiley-Interscience: London and New York, 1972.
(35) Wei, Y.; Hsueh, K. F. *J. Polym. Sci., Part A: Polym. Chem.* **1989**, *27*, 4351.

MA9502258